JOURNAL OF MATERIALS SCIENCE 21 (1986) 571–576

The properties of low-temperature fired piezoelectric ceramics

S. Y. CHENG, S. L. FU, C. C. WEI, G. M. KE
Research Institute of Electronics and Electrical Engineering, National Cheng Kung University, Tainan, Taiwan

Chemicals having relatively low melting points have been used to reduce the required sintering temperature of MnO_2-doped $Pb_{0.9875}((Zr_{0.52}Ti_{0.48})_{0.975}Nb_{0.025})O_3$. Among these compounds Li_2CO_3, Na_2CO_3, B_2O_3, Bi_2O_3 and V_2O_5 are suitable additives for this purpose. The substitution and interstitial properties of the doped ions are discussed in connection with their influences on piezoelectricity and dielectric properties. High Q_m materials and materials with temperature-stability of Q_m could be obtained by Li^+ and B^{3+} or Bi^{3+} doping. Compensation pair effects are proposed to explain the results. Materials exhibiting a Q_m of about 500 with a deviation of less than 10% at temperatures up to 300° C have been prepared for filter use. The sintering temperature is as low as 1070° C.

1. Introduction

The main requirements in the properties of piezoelectric materials for filter application are a high mechanical quality factor Q_m, and temperature and time stability of the resonant frequency [1]. This would also be the basic guideline for the selection of compositions in this research. Nb^{5+} modified $Pb(Zr_{0.52}Ti_{0.48})O_3$ will be called PZTN for simplicity. The two basic compositions in this study are PZTN doped with 0.25 and 0.5 wt % MnO_2.

Special attention has also been paid to a low-temperature fireable process. The so-called liquid phase sintering should be a first candidate for this goal [2]. The required liquid-phase agents have been successfully obtained among Li_2CO_3, Na_2CO_3, B_2O_3, Bi_2O_3 and V_2O_5. By incorporating 0.5 wt % of liquid-phase agent with MnO_2-doped PZTN, the sintering temperature could be reduced to 1070° C. The related characteristics to be discussed are the mechanical Q factor, the planar coupling factor k_p, the resonant frequency f_r and their temperature stabilities. The dielectric properties of the sintered samples will also be discussed to complete the description of Mn^{4+}-doped PZTN.

2. Experimental procedures

A conventional process of ceramic engineering was used. Raw materials of PbO, ZrO_2, TiO_2, Nb_2O_5 and MnO_2 were weighed to obtain the required mole-fractions. After mixing in a ball mill and then drying, the mixture was calcined at 900° C for 2 h. Selected Li_2CO_3, Na_2CO_3, B_2O_3, Bi_2O_3 and V_2O_5 were blended with the calcined powder. A disk-type sample was then formed under 700 kg cm^{-2} pressure. Sintering was performed at 1070° C. The sintering sample was polished and electrodes were fired on both sides of the disk with silver–palladium paste.

The linear shrinkages and densities of the sintered samples were measured to determine the completeness of sintering. Relative dielectric constants and dissipation factors were measured in an HP4270A capacitance bridge. The P–E hysteresis loop was obtained by a Sawyer and Tower circuit. A d.c. field of 3 kV mm^{-1} was applied to polarize the sintered samples. The polarizing temperature was kept at 90° C for at least 30 min. The piezoelectric properties of the samples were measured 24 h after the completion of polarization. Measurement techniques for mechanical Q-factor, coupling factor k_p and resonant frequency f_r were all according to IRE standards [3].

3. Results and discussion

3.1. Effect of additives on the sintering process

The compositions and sintering conditions for different samples are given in Table I. The notation "C.A." stands for equal mole ratio. The properties listed in Table II are for 0.25 wt % MnO_2-doped PZTN with 0.5 wt % Li_2CO_3 and C.A. of Bi_2O_3 as liquid-phase agents. 0.5 wt % MnO_2-doped PZTN with different types of additive and their characteristics are described in Table III.

By comparing the results in Table II with those of

TABLE I Sample treatments and compositions

PZTN + 0.25 wt % MnO_2	
PZTN-1	Sintering at 1070° C for 60 min
PZTN-2	Sintering at 1070° C for 90 min
PZTN-3	Sintering at 1070° C for 120 min
PZTN-4	Sintering at 1070° C for 180 min
PZTN + 0.5 wt % MnO_2	
PZTN-A	0.5 wt % Li_2CO_3 + C.A. Bi_2O_3
PZTN-B	0.5 wt % Na_2CO_3 + C.A. Bi_2O_3
PZTN-C	0.5 wt % Li_2CO_3 + C.A. B_2O_3
PZTN-D	0.5 wt % Na_2CO_3 + C.A. B_2O_3
PZTN-E	0.5 wt % Li_2CO_3 + C.A. V_2O_3
PZTN-F	0.5 wt % Na_2CO_3 + C.A. V_2O_3

0022–2461/86 $03.00 + .12

TABLE II Sintering parameters and room-temperature characteristics for 0.25 wt % MnO_2-doped PZTN

Sample	Density ($g\,cm^{-3}$)	Shrinkage (%)	Porosity (%)	ε_r ($\tan\delta$)	ε_{33}^T ($\tan\delta$)	Q_m	k_p (%)	T_c (°C)	N (kHz mm)
PZTN-1	6.99	7.70	0.67	1078 (5.0)	960 (7.3)	310	47	302	1351
PZTN-2	7.46	8.03	0.32	1001 (2.6)	854 (1.7)	424	43	300	1335
PZTN-3	7.40	8.43	0.20	974 (1.8)	851 (1.3)	340	50	296	1329
PZTN-4	7.24	8.82	0.11	963 (1.1)	856 (0.9)	370	40	295	1324

TABLE III Sintering parameters and room-temperature characteristics of 0.50 wt % MnO_2-doped PZTN

Sample	Density ($g\,cm^{-3}$)	Shrinkage (%)	ε_r ($\tan\delta$)	ε_{33}^T ($\tan\delta$)	Q_m	k_p (%)	N (kHz mm)	T_c (°C)	p_s ($\mu C\,cm^{-2}$)	p_r ($\mu C\,cm^{-2}$)	E_c ($kV\,mm^{-1}$)
PZTN-A	7.71	9.13	1000 (1.0)	803 (0.63)	548	55	1329	286	29.2	19.8	1.14
PZTN-B	7.42	7.53	987 (1.08)	910 (0.73)	380	42	1147	305	15.0	5.5	1.10
PZTN-C	7.64	8.49	946 (1.50)	1009 (0.9)	416	34	1160	360	12.0	5.0	1.62
PZTN-D	7.30	7.71	880 (1.47)	908 (0.79)	280	20	1026	350	15.8	5.3	1.41
PZTN-E	7.62	9.07	882 (6.25)	839 (5.55)	604	20	1433	350	18.4	9.2	1.73
PZTN-F	7.64	8.84	879 (6.8)	795 (6.5)	218	22	1556	343	8.9	4.6	1.40

Table III, it can be seen that 0.5 wt % MnO_2 doping gives a higher Q_m value than 0.25 wt % doping. For this reason, 0.5 wt % MnO_2 doping is preferred in the study of the sloping effects of selected additives. Table II shows that better characteristics are generally obtained after sintering at 1070° C for 90 to 120 min. A longer sintering time gives either a more defective structure by constituent evaporation or a larger grain size, both of which adversely affect the piezoelectricity. For the desired doping effects, the sintering conditions are selected as 1070° C for 2 h. A smaller deviation of the measured results could be obtained by evaluating PZTN-2 and PZTN-3 together with the sintering parameters shown in Fig. 1.

As the sintering progresses, both Li^+ and Bi^{3+} occupy the proper lattice sites to reduce the thermodynamic potential of the lattice. However, a small amount of Li^+ exhibit octahedral interstitial occupation. These effects can be identified in Fig. 2. In Fig. 2a, a longer sintering time gives a small shift of the Curie point toward a lower temperature. This results from the diffusion of impurities into the grain. The interstitial effect with Li^+ can be confirmed by the anomalous increase of dissipation factor when the temperature is higher than the Curie temperature (Fig. 2b). The constriction of volume when the phase changes from a tetragonal to a cubic lattice structure will make the interstitial ions unstable, and the dissipation factor is increased abruptly.

The piezoelectricity and dielectric properties of samples sintered for different times are shown in Fig. 3. Although this shows better dielectric properties for longer times of sintering, the most suitable conditions are 1070° C and 2 h as mentioned above. This

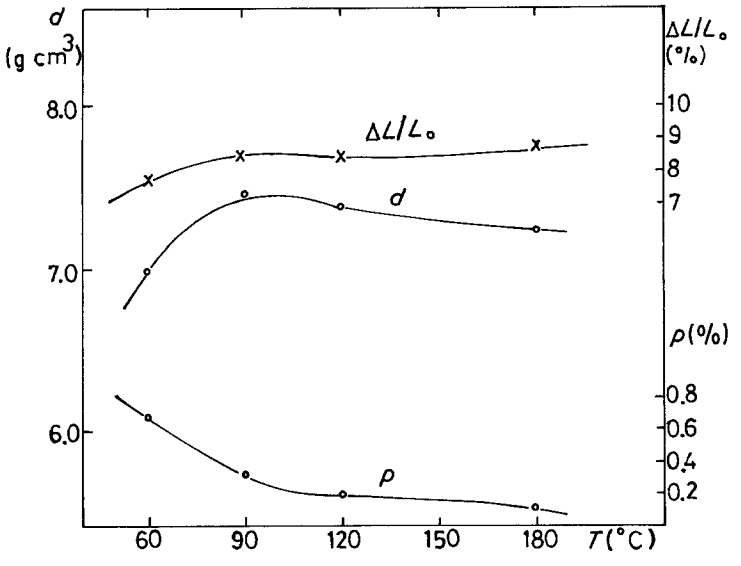

Figure 1 Sintering parameters of 0.25 wt % MnO_2-doped PZTN.

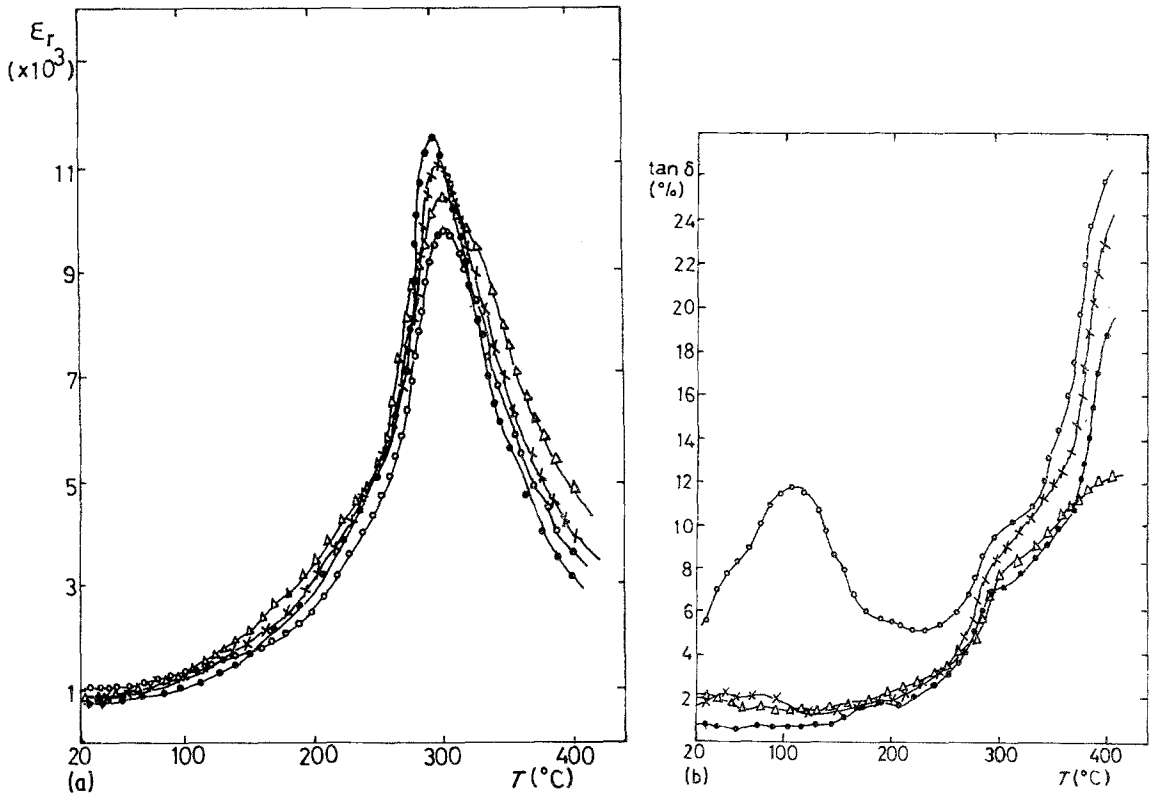

Figure 2 Temperature dependence of (a) dielectric constant and (b) dissipation factor for 0.25 wt % MnO_2-doped PZTN. (○) PZTN–1, (△) PZTN–2, (×) PZTN–3, (●) PZTN–4.

guarantees better properties in both dielectric behaviour and piezoelectricity. The temperature dependences of the piezoelectric characteristics are shown in Fig. 4. Q_m and k_p shows only small variations below 280° C. The comparatively large shift of the resonant frequency needs further improvement if better filtering properties are desired.

In Table III, the characteristics of PZTN doped with selected ions are listed. Li_2CO_3-doped PZTN exhibits a higher density, confirming that liquid-phase sintering is more pronounced with Li_2CO_3 than with Na_2CO_3 doping. V_2O_5 has been proved to be a useful liquid phase during PZT sintering [2], and this is found in PZTN–E and F. The B_2O_3 additive plays a less effective role as a liquid phase because of its relatively low melting point (450° C). Before sintering starts, excessive vaporization of B_2O_3 may interfere with the packing of particles. For mixtures of Li_2CO_3 or Na_2CO_3 with B_2O_3, the results of liquid-phase sintering are shown by PZTN–C and D.

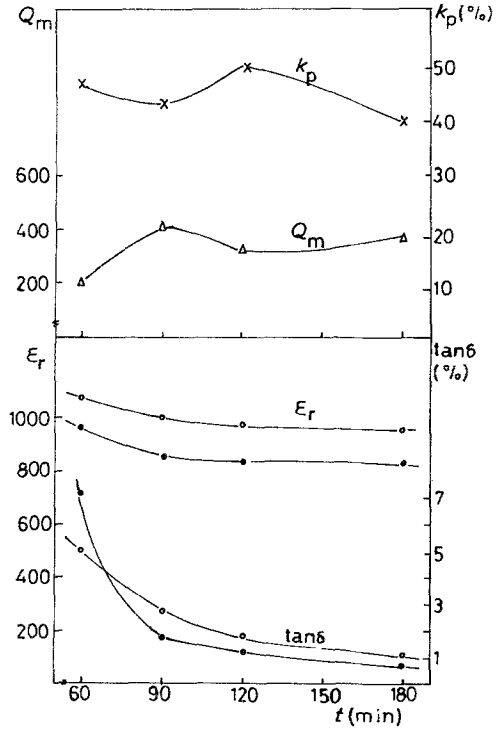

Figure 3 Piezoelectric and dielectric properties of 0.25 wt % MnO_2-doped PZTN; (○) before and (●) after polarization.

3.2. Dielectric characteristics

To evaluate the effect of doping on the desired characteristics, the substituting and interstitial processes of

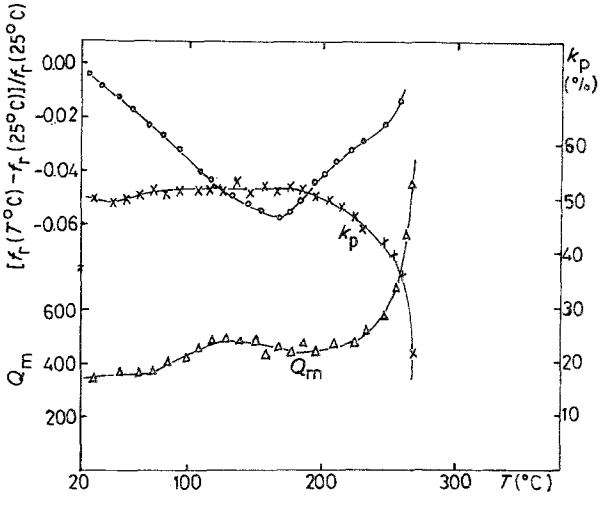

Figure 4 Temperature dependence of piezoelectric characteristics for PZTN–3.

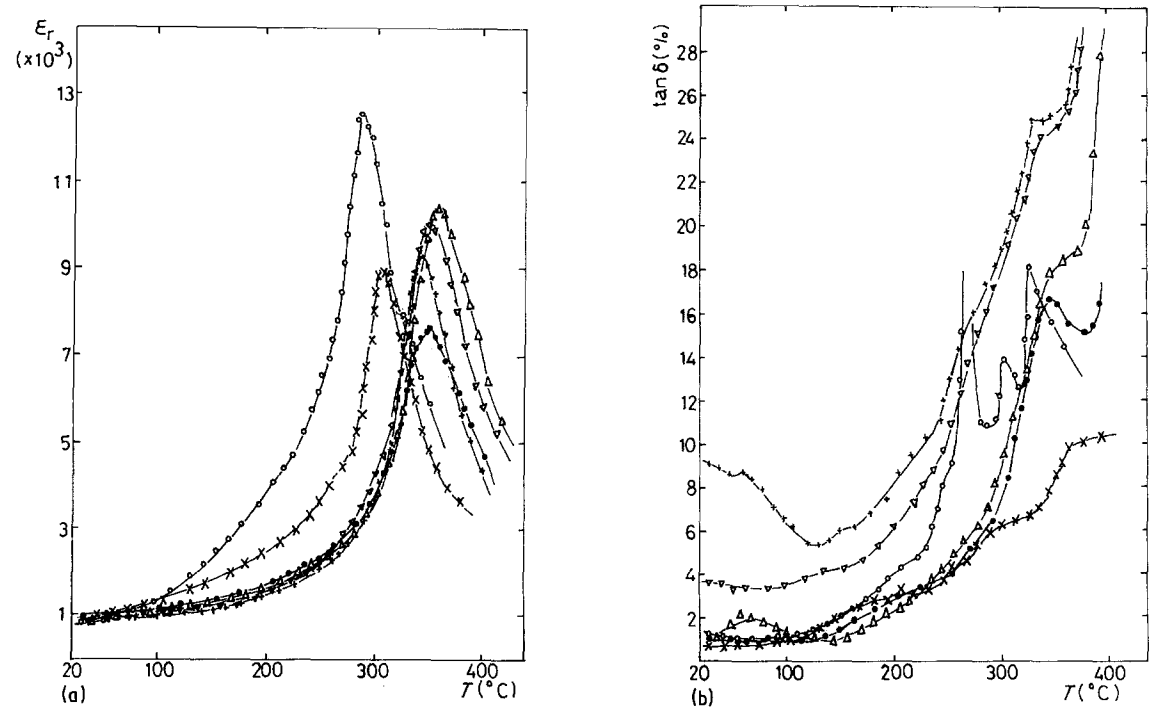

Figure 5 Temperature dependence of (a) dielectric constant and (b) dissipation factor for 0.5 wt % MnO_2-doped PZTN. (○) PZTN–A, (×) TZTN–B, (△) PZTN–C, (●) PZTN–D, (▽) PZTN–E, (+) PZTN–F.

additive ions must be taken into account. There maybe A- or B-site substitution and the possibility of either octahedral or tetrahedral interstitial packing by doping into an ABO_3 perovskite structure. Which effect is dominant will depend on the radius of the doping ion and its chemical properties, such as valency and electronegativity. It is believed that Bi^{3+}, Na^+ and mostly Li^+ undergo A-site substitution, while V^{5+} and mostly B^{3+} undergo B-site substitution [4]. There is some probability of octahedral and tetrahedral interstitial occupation for Li^+ and B^{3+} respectively. Both doping effects depend critically on the method of preparation of the sample, and would alter the characteristics in many ways.

The observed dielectric characteristics can be divided into three groups: (a) high ε_r with low $\tan\delta$ value, (b) medium ε_r and $\tan\delta$ but ε_r increases after polarization, and (c) low ε_r with high $\tan\delta$ value. In (a), ε_r decreases slightly compared with that of undoped PZTN, suggesting A-site substitution of Li^+, Na^+ and Bi^{3+}. The lowering of the Curie point also confirms this point of view [5]. In (b), the small B^{3+} ion probably has interstitial occupation. Polarizing treatment creates a slight shift of B^{3+} relative to its position before polarizing. A higher dipole moment contributes to an increase of ε_r and a decrease of $\tan\delta$ as shown. The higher coercive field also supports this opinion. Conversely, if B^{3+} replaced the B-site ion and acted as an acceptor, this would increase the dissipation factor and lower the T_c (Curie point) value. It is therefore concluded that B^{3+} doping mostly has an interstitial occupation rather than substitution at the B-site. On the other hand, V^{5+} in (c) is considered as a donor for B-site substitution [2]. The high value obtained for $\tan\delta$ may be ascribed to the over-compensation of simultaneous B-site Nb^{5+} doping. This effect may enforce the interstitial doping of Li^+ because of its rather smaller ionic radius (0.060 nm) compared with Pb^{2+} (0.120 nm). The effect would be the same for Na^+ (0.095 nm) doping. Further examples are shown in Fig. 5. Arising from the interstitial ions, increased temperature gives more vibrating energy to the lattice ions and increases in $\tan\delta$ would be expected; this is obvious for samples of PZTN–E and F.

3.3. Piezoelectric characteristics

The piezoelectric characteristics are also listed in Table III. The substituting and interstitial occupation of doping ions determine the piezoelectric properties of a sample. In general, the substitution of ions with different ionic sizes would distort the tetragonality of the lattice structure. Phase shifts towards or away from the ferroelectric phase depend on the Goldschmidt tolerance factor t. An increasing t value represents a more ferroelectric-like property, but a decreasing t value would enhance the antiferroelectric phase [6]. It is shown that the better piezoelectric properties of PZTN–A and B are the result of less distortion of tetragonality. The relatively high k_p and Q_m values of PZTN–A are attributed to the higher c/a ratio of the lattice determined by X-ray diffraction analysis [4]. The higher c/a ratio may be a response to interstitial occupation by the Li^+ ion. In PZTN–C, D, E and F, the small cations substituted at the A- or B-site reduce the tolerance factor t. A shift toward the antiferroelectric phase causes decreases in p_s and p_r, but an increase in E_c [7].

Figs. 6 and 7 show the temperature dependence of Q_m and k_p. The anomalous behaviour of Q_m for PZTN–E may be explained by an interaction between interstitial Li^+ and V^{5+} substitution in the B-site, or the interaction between interstitial Li^+ and an A-site vacancy. The interactions would become obvious on increasing the temperature. These interactions provide another source of internal friction and thus reduce the Q_m value [8]. It is known that the antiferroelectric

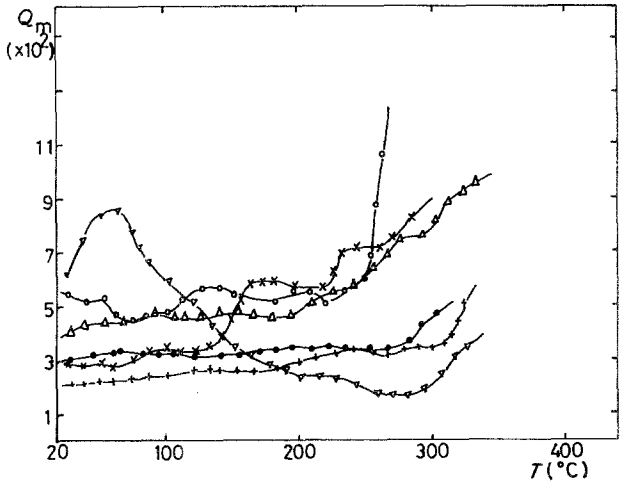

Figure 6 Temperature dependence of Q_m for 0.5 wt % MnO_2-doped PZTN. (○) PZTN–A, (×) PZTN–B, (△) PZTN–C, (●) PZTN–D, (▽) PZTN–E, (+) PZTN–F.

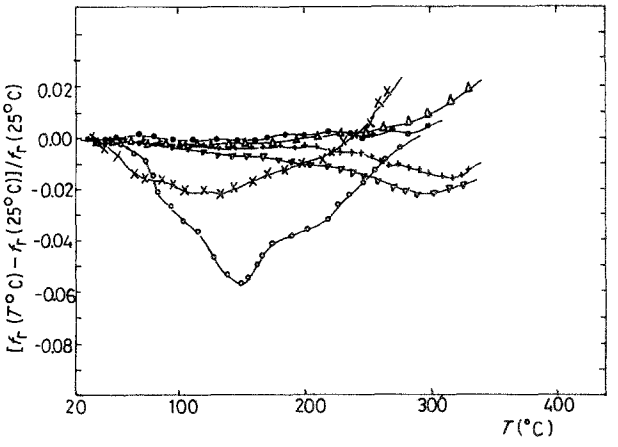

Figure 8 Temperature dependence of resonant frequency for 0.5 wt % MnO_2-doped PZTN. (○) ZPTN–A, (×) PZTN–B, (△) PZTN–C, (○) PZTN–D, (▽) PZTN–E, (+) PZTN–F.

phase is more stable than the ferroelectric phase. Temperature-stable Q_m and k_p values are obtained in PZTN–C, D and F. This stability is also seen in Fig. 8. PZTN–C, D and F show a relatively small variation of resonance frequency up to 300° C. The larger variations observed in samples of PZTN–A and B are typical results for ferroelectric materials. This also confirms the A-site substitution suggestion mentioned before. In Fig. 9, the *P–E* hysteresis of sample PZTN–D shows a slightly double-looped shape. This demonstrates that the phase shift is again toward the antiferroelectric phase.

4. Conclusions

Li_2CO_3, Na_2CO_3, B_2O_3, Bi_2O_3 and V_2O_5 are suitable additives for the preparation of low-temperature fireable piezoelectric materials. In order to improve the properties a compensation pair, usually consisting of a monovalent ion and an equal amount of trivalent ion, is introduced to determine the charge balance of doped PZTN. A-site occupation is dominant for Li^+, Na^+ and Bi^{3+} doping, but V^{5+} and B^{3+} facilitate B-site substitution.

An interstitial process for small cations has to be considered for both octahedral and tetrahedral interstitial occupation. It seems that Li^+ prefers octahedral and B^{3+} both octahedral and tetrahedral occupancy. This process is critically dependent on the accompanying dopant, and would alter the piezoelectric and dielectric characteristics in many ways. It may be that because of the versatility of B^{3+} doping, Li^+–B^{3+} and Na^+–B^{3+} doping pairs show better properties for filter use.

An enforced ferroelectric–antiferroelectric transition is found with the substitution of small cations. This would adversely affect the piezoelectric properties and should be minimized. It is also because of this effect that an interstitial process of doping is preferred to a substitution process.

Depending on the field of potential applications of piezoelectric materials, these low-temperature sinterable doped-PZTN materials are divided into three groups: (a) high Q_m for filter use, such as PZTN–A and E; (b) high k_p for use in electromechanical coupling devices, such as PZTN–A and B; and (c) more temperature-stable materials for critical filter design use, such as PZTN–C and D. All materials have ε_r ranging from 900 to 1000, together with tan δ less than 1.5%. The smallest deviation of Q_m and f_r could be less than 10 and 5% respectively. The sintering temperature is 1070° C or lower.

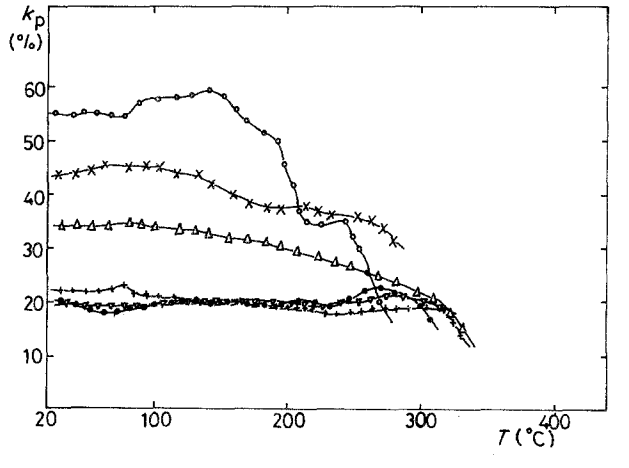

Figure 7 Temperature dependence of k_p for 0.5 wt % MnO_2-doped PZTN. (○) PZTN–A, (×) PZTN–B, (△) PZTN–C, (●) PZTN–D, (▽) PZTN–E, (+) PZTN–F.

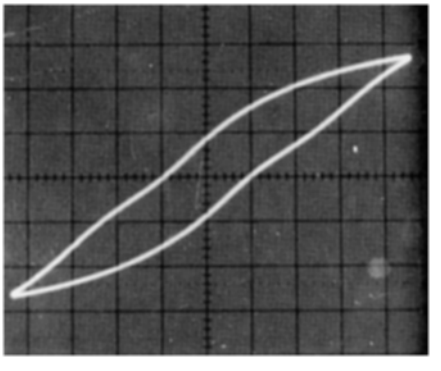

Figure 9 P–E hysteresis of PZTN–D.

References

1. F. KULCSAR, *J. Amer. Ceram. Soc.* **42** (1959) 343.
2. D. E. WITTMER, *ibid.* **64** (1981) 485.
3. H. JAFFE, *Proc. IRE* **49** (1961) 1161.
4. T. YAMAMOTO, H. IGARASHI and H. OKAJAKI, *J. Amer. Ceram. Soc.* **66** (1983) 363.
5. C. P. SMYTH, "Dielectric Behavior and Structure" (McGraw-Hill, 1955), Chap. 5.
6. P. GONNARD and M. TROCCAZ, *J. Solid State Chem.* **23** (1978) 321.
7. S. TAKAHASHI, *Ferroelectrics* **41** (1982) 143.
8. V. S. POSTNIKOV, V. S. PAVLOV and S. K. TURKOV, *J. Phys. Chem. Solids* **31** (1970) 1785.

Received 24 October 1984
and accepted 29 March 1985